J. Micromech. Microeng. **19** (2009) 074008 (11pp) doi:10.1088/0960-1317/19/7/074008

Fabrication technology for silicon-based microprobe arrays used in acute and sub-chronic neural recording

S Herwik[1], S Kisban[1], A A A Aarts[2,3], K Seidl[1], G Girardeau[4], K Benchenane[4], M B Zugaro[4], S I Wiener[4], O Paul[1], H P Neves[2] and P Ruther[1]

[1] Department of Microsystems Engineering (IMTEK), University of Freiburg, Freiburg, Germany
[2] Interuniversity Microelectronics Center (IMEC), Leuven, Belgium
[3] Catholic University of Leuven, ESAT-MICAS, Leuven, Belgium
[4] Laboratoire de Physiologie de la Perception et de l'Action (LPPA), Collège de France, CNRS, Paris, France

E-mail: herwik@imtek.de

Received 19 December 2008, in final form 15 April 2009
Published 30 June 2009
Online at stacks.iop.org/JMM/19/074008

Abstract
This work presents a new fabrication technology for silicon-based neural probe devices and their assembly into two-dimensional (2D) as well as three-dimensional (3D) microprobe arrays for neural recording. The fabrication is based on robust double-sided deep reactive ion etching of standard silicon wafers and allows full 3D control of the probe geometry. Wafer level electroplating of gold pads was performed to improve the 3D assembly into a platform. Lithography-based probe-tracking features for quality management were introduced. Probes for two different assembly methods, namely direct bonding to a flexible micro-cable and platform-based out-of-plane interconnection, were produced. Systems for acute and sub-chronic recordings were assembled and characterized. Recordings from rats demonstrated the recording capability of these devices.

(Some figures in this article are in colour only in the electronic version)

1. Introduction

Wire electrodes have been a versatile tool for neuroscientists for decades [1]. They have allowed the first recordings of extracellular neural activity from the brain in close proximity to firing neurons. Wire electrodes are robust and offer excellent recording capabilities, as is necessary for studies contributing to the basic understanding of the central nervous system (CNS). However, for advanced studies of neural clusters and neuron populations it is necessary to record from a large number of firing neurons within a defined brain volume. The potential of wire electrodes for such applications is limited, since they offer only a single recording site per wire, which as a consequence would require a large number of electrodes to be inserted into the neural tissue. Besides single wires, rather specific wire assemblies such as multi-wire electrodes with a probe diameter of 350 μm have been reported [2]. However, the multi-wire electrodes as well as single wire electrodes are hand-made at a high labor cost for fabrication and suffer from a low reproducibility of the electrode characteristics, such as their impedance.

Starting with the pioneering work from Wise *et al* [3], silicon-based electrode arrays have been developed in the past with the goal of an increased number of recording sites, among other improvements. A wide variety of systems has been realized using microsystem technologies [4–12]. Some of them have even been brought to market (NeuroNexus Technologies, Ann Arbor, MI, USA, and Blackrock Microsystems, Salt Lake City, UT, USA). The corresponding fabrication processes are based on the wet [3–9] or dry etching [10–12] of silicon. Particularly well known are the Michigan probes [3–7] and the Utah array [8, 9] that have found a wide range of applications. The Utah array comprises 10 × 10 out-of-plane micro-needles protruding

from a slim backbone [8]. Each micro-needle carries one recording site at its tip. The structure is compatible with the hybrid integration of CMOS electronics on the rear of the backbone [9]. In addition, with their conical shape, the micro-needles are mechanically robust. Limitations of these systems include the fact that only a single tip-electrode is available per shaft, similar to the wire electrodes, and the difficult insertion of the 100 relatively densely packed probe shafts. In contrast, the Michigan probes utilize a technology allowing three-dimensional (3D) arrays to be obtained by assembling two-dimensional (2D) probe combs into 3D structures [5–7]. The backends of those neural probe versions containing CMOS circuitry are either oriented vertically [5] or horizontally [6] with respect to the assembly platform, which affects the footprint of the devices. In contrast, the neural probe systems described in [7] comprise CMOS circuitry in the platform rather than on the probe array. Nonetheless, the subdural application of these devices is rendered difficult by the bulky backbone containing the CMOS electronics. With a thickness of only 15 μm, the probe shafts are highly flexible. Although this is an advantage in view of reduced tissue damage during insertion and long-term biotolerability, skilled personnel are required to insert these delicate devices.

This study presents a new fabrication technique for silicon-based neural probes and their assembly into multifunctional probe arrays. The probes offer the advantages of both approaches described above, i.e. multiple electrodes per shaft and unrestricted freedom in the 2D probe layout as in the case of the Michigan probes as well as high probe robustness and a slim backbone in the case of the 3D arrays and the possibility for a hybrid integration of circuitry underneath the probe platform as in the case of the Utah array. In comparison to existing 3D arrays based on needle combs [5–7], the total height of the array backbone which remains above the brain surface after implantation can be kept well below 500 μm. This is crucial for the realization of floating devices in view of space constraints in chronic applications, where the array is implanted and covered with dura mater and artificial bone. Additionally, our fabrication process allows CMOS circuitry to be integrated directly on the probe shaft enabling the integration of a large number of electrodes with a minimal inter-electrode distance. In contrast, the integration of circuitry on probe shafts has not yet been demonstrated for Michigan probes, likely due to their fabrication based on high-density boron diffusion combined with wet etching. Further, the probe thickness can be adjusted during fabrication, with the goal of achieving a satisfactory compromise between minimal tissue damage during implantation and probe stiffness required to reliably implant the array without probe shaft buckling. Lastly, the use of standard bare silicon wafers and CMOS substrates is made possible, in contrast to more expensive silicon-on-insulator (SOI) wafers as used, e.g., in [10] and [12].

The neural probe structures were developed in the framework of the EU-project NeuroProbes [13, 14]. They comprise probes for electrical recording and stimulation as well as drug delivery using integrated fluidic micro-channels [15]. Chemical sensing using amperometric biosensors [16] and electronic depth control using CMOS circuitry integrated in the probe shafts [17, 18] are further features. The multifunctional probes are suited for mechanical assembly into a slim common backbone and the electrical connection into this base structure. Alternatively, they may be connected to flexible ribbon cables. The fabrication technology of the probes is based on deep reactive ion etching (DRIE) of standard silicon wafers, in contrast to [10] and [12]. The post-CMOS compatibility of this fabrication approach is demonstrated in [18]. Probes with lengths of up to 8 mm and probe combs up to four shafts comprising nine electrodes per shaft were fabricated and tested *in vivo* [19].

In the following, the probe layout is presented in section 2. The fabrication and assembly are discussed in detail in section 3. Finally the *in vivo* recording capability of the probes is demonstrated in section 4.

Table 1. Types of neural probes for different assembly schemes and shaft lengths.

Type	No of shafts	Electrodes per shaft	Shaft length L_S (mm)
Cable	1, 4	9	2, 4.5, 8
Platform	4	5	2, 4.5, 8

2. Probe layout

The neural probes schematically shown in figure 1 comprise slender needle-like probe shafts attached to a probe base serving for electrical and mechanical interconnection. Planar electrodes along the probe shafts are connected to contact pads on the probe base by metal leads. The probes were designed as single shaft elements or as combs comprising four parallel shafts of equal length. While single shaft probes can be used in combination with a highly flexible ribbon cable [19], probe combs with different probe base layout can be assembled either with a ribbon cable [20] or on a slim platform [21] as illustrated in figures 1(*a*) and (*b*), respectively. In addition, probes of the cable variant lend themselves for connection to a custom designed printed circuit board (PCB) for acute applications similar to the systems commercialized by NeuroNexus. Figure 2(*a*) shows the examples of layouts of a probe comb for cable assembly. The structures are available as one-dimensional (1D), 2D and 3D probe assemblies employing single-shaft probes with nine electrodes, probe combs with 36 electrodes and two combs assembled rear-to-rear comprising 72 electrodes, respectively. The platform probes contain five electrodes per shaft and thus 20 electrodes per comb. An example is shown in figure 2(*b*). With four combs per platform, the platform-based 3D probe arrays comprise 80 electrodes in total [21]. Probes for the different interconnection schemes and with different probe lengths of 2 mm, 4.5 mm and 8 mm, fabricated so far and currently available for *in vivo* testing, are listed in table 1. The probe variants shown in figure 2 have shaft lengths of 2 mm. The probes are suspended in the fabrication wafer by thin struts located on each side of the probe bases as indicated

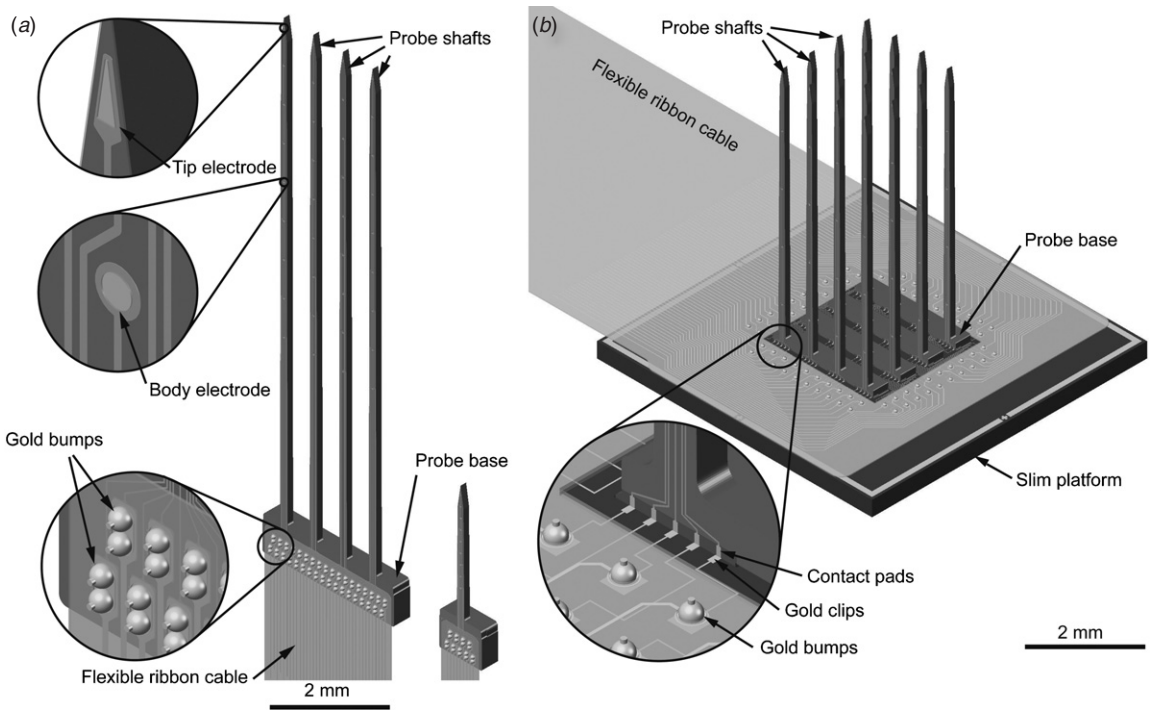

Figure 1. Schematic of probe assemblies: (*a*) probes with four shafts and with a single shaft directly connected to a highly flexible ribbon cable and (*b*) slim platform-based 3D-probe array with 4 × 4 shafts.

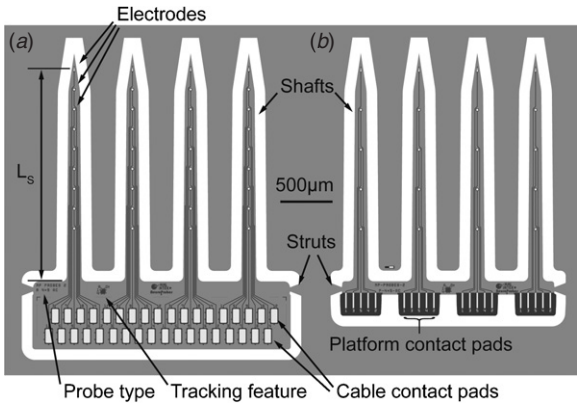

Figure 2. Layout of the 2 mm long four-shaft probes with different assembly variants; probes for (*a*) cable and (*b*) platform-based assembly.

in figure 2. They can be snapped off the wafer by applying a torsional force, thus breaking the struts.

The probe bases of the single-shaft and the four-shaft probes for cable assembly measure 790 × 640 μm^2 and 2440 × 640 μm^2, respectively. They comprise contact pads with dimensions of 60 × 130 μm^2 and the tracking features. The contact pads are electrically connected to a highly flexible polyimide ribbon cable using the *MicroFlex* technology [22]. The thickness of the base is equal to the full wafer thickness, i.e. 300 μm. Similarly the probe base of the platform variant shown in figure 2(*b*) is 300 μm thick, but it is 2020 × 325 μm^2 in size. It comprises four segments of 400 × 200 μm^2, each containing five electroplated gold contact pads (15 × 150 μm^2, thickness 3 μm) for electrical interconnection to the slim platform. The segments of the probe base fit into respective bays on the platform using the interconnection technique described in [23]. Gold clips hanging over the bay edges of the platform ensure the electrical connection between probe and platform. The clips are bent down during assembly and pressed against the contact pads on the probe base.

The probe shafts are slightly tapered, with a width of 140 μm at the base narrowing down to roughly 100 μm toward the shaft end. The shaft ends by a sharp tip with an opening angle of 17°. In the case of both comb versions, i.e. for cable and platform assembly, the distance between individual shafts is set to 550 μm. So far, shaft thicknesses of 100 μm and 80 μm were achieved using the fabrication process detailed in section 3.

As illustrated in figure 1(*a*), one triangular tip electrode as well as four or eight circular body electrodes with a diameter of 20 μm are equidistantly arranged along the probe shaft variants for platform and cable assembly, respectively. The electrode area in contact with tissue is 314 μm^2 for both electrode geometries. Metal leads with a width and spacing of 5 μm connect the electrodes to the corresponding contact pads on the probe base.

2.1. Probe tracking

Each probe carries a unique identifier comprising probe type and wafer number for tracking of fabrication batches. Although laser writing is widely used in industry to identify individual dies for quality management, it cannot be realistically applied in the case of the neural probes. The reason is the limited area available on the probe base, in particular of the probes intended for platform assembly. As a

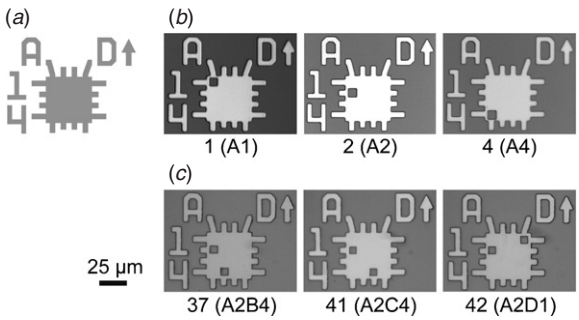

Figure 3. (*a*) Grid used for the wafer code for probe tracking. Micrographs of wafer codes with (*b*) one and (*c*) two dots realized on six different wafers with the corresponding coded serial number.

consequence a photolithographically defined pattern encoding the desired information was developed. The wafer code consists of a 2D grid 80 × 80 μm^2 in size defining columns A through D and lines 1 through 4 as shown in figure 3(*a*). One or several square dots with a size of 10 × 10 μm^2 are patterned into this grid, thus allowing $N_1 = 4 \times 4 = 16$, $N_2 = 16 \times 15/2! = 120$, $N_3 = 16 \times 15 \times 14/3! = 560$, etc, individual wafers to be identified when one, two, three, etc, dots are employed. The values N_i are the number of possible dot combinations with $i = 1, 2, 3$, etc, dots per wafer code. In the present work, we included single dots and binary dot combinations, as illustrated in figures 3(*b*) and (*c*), respectively. The realization of these tracking features is based on but not limited to the lift-off process of the probe metallization as described in section 3.

3. Fabrication and assembly

3.1. Fabrication process

The fabrication process uses eight masks. It relies heavily on deep reactive ion etching (DRIE) of silicon. The probes are realized on 4 inch, double-side polished, p-doped (1 0 0) silicon wafers with a thickness of 300 μm. In a first step, an insulating layer is deposited on both wafer sides. The layer is a stress compensated stack of a thermal silicon dioxide (SiO_2) grown at 950 °C, a silicon nitride (Si_3N_4) produced by low-pressure chemical vapor deposition (LPCVD) at 770 °C and a LPCVD low temperature oxide (LTO) deposited at 425 °C. The corresponding thicknesses are 200 nm, 100 nm and 200 nm. Figure 4(*a*) shows that an additional layer is then deposited on the wafer rear. The layer is a 4.6 μm thick stress compensated stack of SiO_x and Si_xN_y deposited using plasma enhanced chemical vapor deposition (PECVD). It serves as the masking layer during the subsequent DRIE step. The stress compensation of the different layer stacks is based on residual stress values reported in [24] and [25]. Tables 2 and 3 summarize the mechanical properties of the applied dielectric thin-film materials and the composition of the different layer stacks.

The electrode metallization consists of 30 nm titanium (Ti), 200 nm gold (Au), 100 nm platinum (Pt) and 30 nm Ti. These layers are deposited by evaporation and patterned

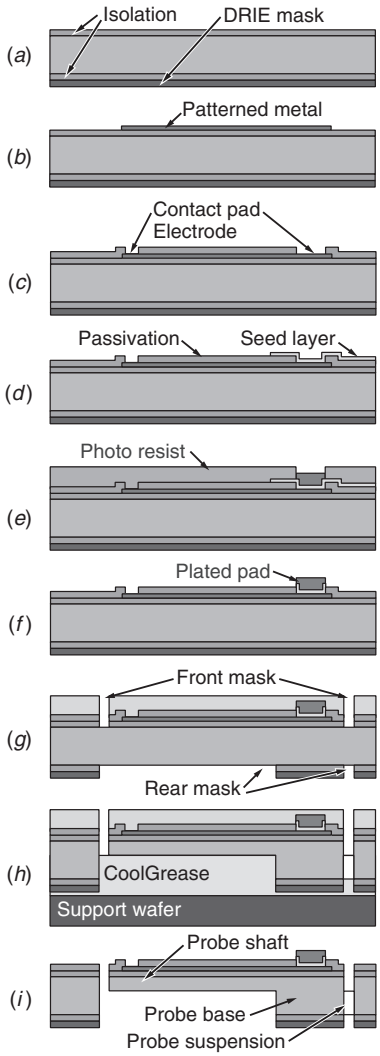

Figure 4. Fabrication process for silicon probes, comprising (*a*) deposition of insulation and masking layers; (*b*)–(*d*) deposition and patterning of metallization, passivation layer and seed layer; (*e*), (*f*) electroplating, photoresist stripping and seed layer etching; (*g*) patterning of dielectric masking layers using RIE and (*h*) DRIE from wafer rear and front using a support wafer; and (*i*) unmounting from the support wafer and cleaning.

using a lift-off process. The result is schematically shown in figure 4(*b*). The lift-off process applies the image reversal photoresist *AZ5214E* from Clariant, Switzerland. The evaporation was performed in a static deposition mode with the wafer position fixed above the evaporation source. By this choice frayed metal edges are avoided. In contrast, in the alternative dynamic mode, where up to six 4″ wafers are rotated above the crucibles, the negatively tapered resist sidewalls are partly covered due to an increased angle of incidence. While titanium serves as the adhesion layer to the dielectric thin films, gold is used to minimize the interconnection resistance and platinum is the electrode material of choice. The metal stack is covered by a 1.5 μm thick passivation multilayer. This is again a stress compensated layer stack of alternating PECVD SiO_x and Si_xN_y thin films with thicknesses listed in table 3. The passivation is patterned by reactive ion etching (RIE) using the *STS RIE Multiplex* etcher of Surface

Table 2. Residual stress of dielectric layers applied as insulation, passivation or etch mask [24, 25]. Process parameters: SiO_2, wet oxide grown at $T_{dep} = 950$ °C; LPCVD Si_3N_4 $T_{dep} = 770$ °C; LTO, $T_{dep} = 425$ °C; PECVD layers, $T_{dep} = 300$ °C, RF frequency 13.56 MHz, RF power 30 W, $p = 900$ mTorr; SiO_x, N_2 392 sccm, N_2O 1420 sccm, SiH_4 10 sccm; and Si_xN_y, N_2 1960 sccm, SiH_4 40 sccm, NH_3 55 sccm.

Material	Residual stress (MPa)
Thermal silicon dioxide SiO_2	-318 ± 15
LPCVD silicon nitride Si_3N_4	$+1194 \pm 30$
Low temperature silicon oxide LTO	-321 ± 15
PECVD silicon oxide SiO_x	-312 ± 16
PECVD silicon nitride Si_xN_y	$+412 \pm 28$

Technology Systems, UK, thus opening electrodes and contact pads, as indicated in figure 4(*c*). A RIE recipe optimized for the etching of SiO_2 with a platen power of 219 W; a process pressure of 100 mTorr; and gas flows of 15 sccm, 35 sccm and 50 sccm, for tetrafluoromethane (CF_4), fluoroform (CHF_3) and argon, respectively, is applied. As the dry etching stops at the Ti surface, Pt is protected against the CF_4/CHF_3 plasma. A subsequent wet etching of the upper Ti on the electrodes and contact pads in 1% hydrofluoric acid (HF) exposes the Pt electrodes. The successful removal of the Ti layer is verified by an activity test exploiting the decomposition of hydrogen peroxide (H_2O_2) on Pt, resulting in the formation and observation of O_2 bubbles. In contrast, no H_2O_2 decomposition is observed on dielectric, Ti and Au surfaces. To facilitate the wetting of small features, i.e., the recessed electrode surfaces, the wet etching and H_2O_2 activity test is preceded by an isopropyl alcohol dip.

The next step is the electroplating of the contact pads of the platform combs. For this purpose, a seed layer is first patterned using the sputter deposition of titanium–tungsten (TiW, 30 nm) and gold (100 nm) and a lift-off process using again the *AZ5214E* photoresist. The result is illustrated in figure 4(*d*). The seed layer patterning is required to prevent its deposition on the exposed electrodes. The electroplating is performed using a 5 μm thick *AZ4533* photoresist from Clariant, Switzerland, acting as a mask, and the electrolyte *Puramet* 202 from AMI-Doduco, USA, at 58 °C. The current density is set to 20 A m^{-2} for 20 min to achieve a layer thickness of about 4 μm. As shown in figure 4(*e*), the openings in the thick photoresist are thereby partially filled.

After photoresist stripping, the remaining Au seed layer and the TiW adhesion layer around the contact pads are wet etched using a potassium iodide and iodine (KI/I_2) solution and 30% H_2O_2 at 40 °C, respectively. Such processing results in a passivation surface cleared of metal, as schematically shown in figure 4(*f*).

The order of the subsequent fabrication steps was changed in comparison to the previously reported technology [19] to avoid wafer fracture during the dry etching steps. First both rear and front SiO_x/Si_xN_y etch masks are patterned using RIE. As indicated in figure 4(*g*), the photoresist on the wafer front is left as a protection of the electrode surfaces and the contact pads against the subsequent etch steps. Then, the overall geometry of the probes and the shaft thickness are defined from the wafer rear in a first DRIE step using an *STS ICP Multiplex* etcher from Surface Technology Systems, UK. Probes as thin as 80 μm were realized. As the DRIE rate is dependent on the mask layout, i.e. the amount of open area, and on the position on the wafer, variations in the etch depth can be expected. In order to minimize these effects, the etch mask open area was designed to be as homogeneous as possible across the wafer (cf figure 5(*a*)). Further, a DRIE process specified by the ICP supplier to offer an etch homogeneity of 5% over 4 inch wafers was applied. With these measures, shaft thickness variations within ± 5 μm were achieved at a total etch depth of 200 μm. This variation has a negligible impact on the functioning of the probe.

The probe wafer is then mounted onto a solid support wafer by means of the heat conductive paste *Cool Grease 7016* from AI Technology Inc., USA, as illustrated in figure 4(*h*). The mounting serves three purposes: (i) the etch selectivity between silicon and photoresist is increased due to an optimal wafer cooling using the heat conductive paste, (ii) the delicate rear-etched probe wafer is mechanically stabilized and (iii) air entrapment between support and probe wafers is avoided as the heat conductive paste fills the etched cavities on the wafer rear. This filling of the cavities is particularly important as the high vacuum and the temperature increase during RIE and DRIE would cause the expansion of trapped air bubbles in the recessed etch cavities. In the past, this has been responsible for wafer fracture and a decreased fabrication yield of about 60%. The final DRIE step is performed from the wafer front to complete the release of the probes. The fabrication wafer with probes suspended by a pair of thin struts is finally separated from the support wafer. The heat conductive paste is easily dissolved in acetone applying megasonic cleaning using a submersible 1 MHz transducer from SONOSYS Ultraschallsysteme GmbH, Germany, at a power level of 500 W for 10 min. Delicate mechanical features

Table 3. Layer composition and thickness-averaged residual stress of layer stacks used as insulation, passivation or etch mask.

Layer stack	Layer material	Thickness (nm)	No of layers	Stack thickness (nm)	Residual stress (MPa)
Insulation	SiO_2	200	1	500	-16.8
	Si_3N_4	100	1		
	LTO	200	1		
Masking layer	SiO_x	325	8	4600	2.78
	Si_xN_y	250	8		
Passivation layer	SiO_x	210	4	1480	1.06
	Si_xN_y	160	4		

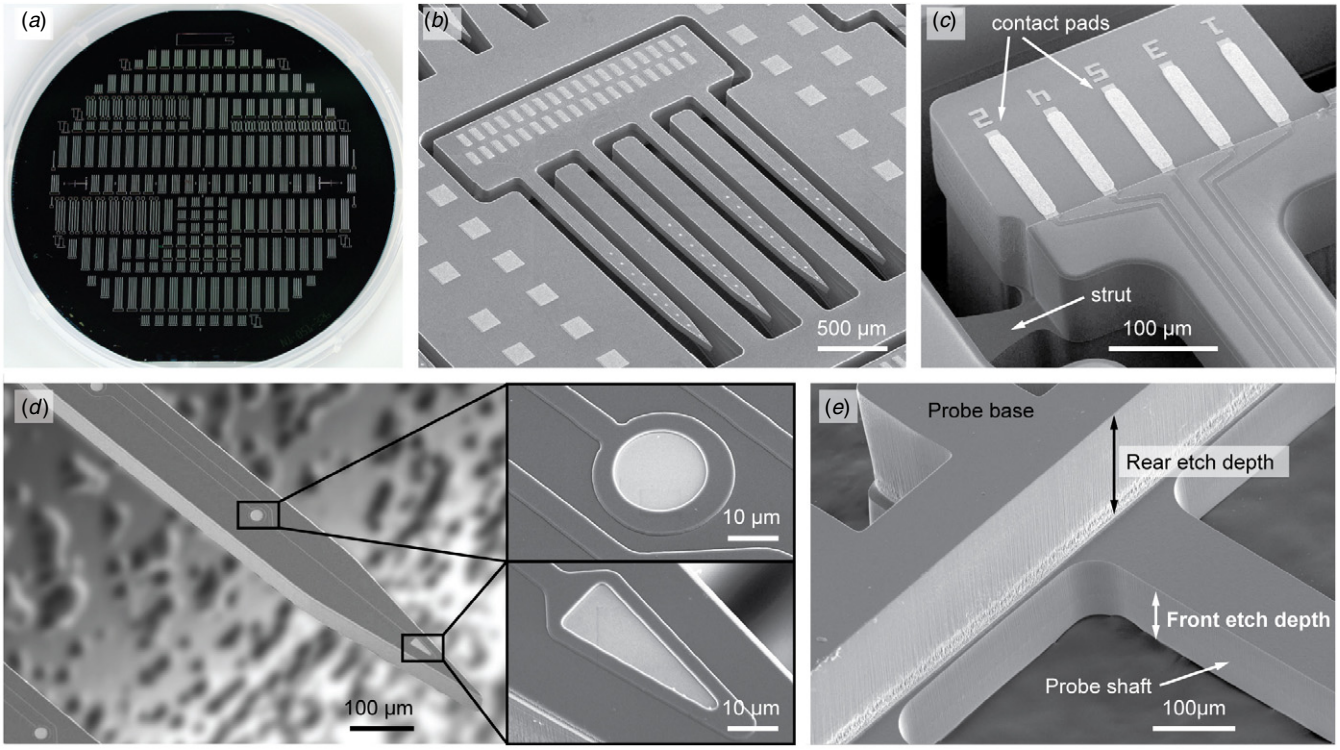

Figure 5. (*a*) Photograph of a wafer with suspended single shaft and comb-based probes. Scanning electron micrographs of (*b*) a 2 mm long shaft for cable assembly, (*c*) a probe base with contact pads for the platform and probe suspension (struts), (*d*) the tip region of a probe shaft with enlarged views to the body and tip electrodes and (*e*) the backside of the probe showing the probe base with a thickness of 300 μm and the probe shaft with a thickness of 100 μm.

survive this procedure without any harm. The individual probes are twisted off the wafer by gentle torsion breaking the thin struts. The resulting structure is shown in figure 4(*i*). The overall yield of the fabricated wafers is currently 100%.

A photograph of a fabricated probe wafer with suspended single-shaft and four-shaft probes is shown in figure 5(*a*). A scanning electron micrograph of a four-shaft probe for cable assembly with four 2 mm long shafts suspended in the fabrication wafer is presented in figure 5(*b*). Figure 5(*c*) shows a probe base for platform assembly with electroplated pads and suspension struts on the wafer rear as indicated, and figure 5(*d*) demonstrates details of a probe shaft with a tip-like electrode and three circular body electrodes. A rear view of the probe is illustrated in figure 5(*e*); the step from the rear surface of the probe base to the probe shaft corresponds to the rear etch depth as indicated; it defines the probe shaft thickness.

3.2. Wafer code

The realization of the wafer code requires one further dark field mask termed *Code* and as many additional UV exposures as dots are to be written into the code grid. These exposures have to be performed during the photolithography step to define the electrode metal pattern and before the image reversal baking step, flood exposure and development of the photoresist. For every probe, the probe-type identification and the grid layout for the wafer code are implemented in the lithography mask termed *Metal* used for defining all electrode, interconnection and pad structures. The probe-type identification consists of the layout name, the probe variant identification and a running number. The procedure for patterning the electrode metallization layer into the electrodes, interconnection, pads and the wafer number codes comprises the following individual steps: (i) photoresist spin coating and soft bake, (ii) mask alignment and UV exposure using the *Metal* mask, (iii) mask alignment of *Code* mask, (iv) relative shift of the *Code* mask in steps of 10 μm in the x- and y-directions to the desired grid positions followed by UV exposure and (v) post-exposure bake, flood exposure for image reversal and resist development. In the case of two or more dots per grid, process steps (iii) and (iv) are repeated. In this way, dots of resist are defined using the *Code* mask inside of the grid areas defined by the *Metal* mask. These dots remain free of metal as shown in figures 3(*b*) and (*c*). The resulting pattern is small enough to fit on every probe base.

3.3. Assembly process

The electrical connection between probes or the slim platform and external circuitry is performed using highly flexible polyimide (PI) ribbon cables. These cables consist of two 5 μm thick PI layers with a Pt metallization sandwiched in between. The ends of the Pt lines of the cable are layouted as rounded rectangles with circular openings. Both PI layers comprise corresponding vias with different opening diameters r_1 and r_2 as shown in the cross-sectional view in figure 6(*a*). The mechanical and electrical connections between probes and cables are realized applying the *MicroFlex* Technology [22]. As schematically shown in figure 6(*b*), the openings in

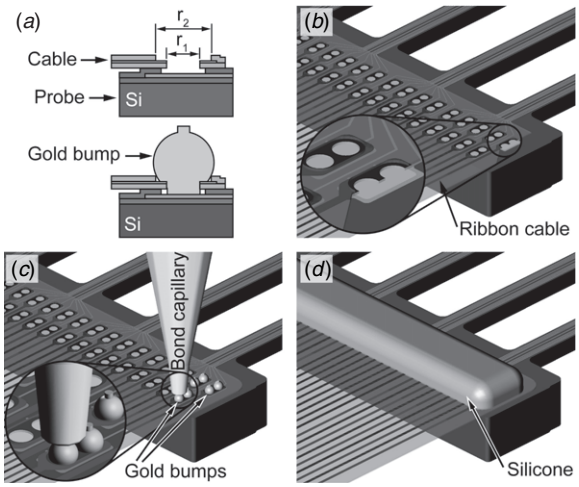

Figure 6. Interconnection of the probe with the ribbon cable. (*a*) Cross-section of the silicon structure and the ribbon cable: the openings in the top and the bottom PI layers have diameters r_1 and r_2, respectively; (*b*) alignment of the cable: the line ends on the cable are realized as rectangles with circular openings. Both polyimide layers have openings at the corresponding positions (inset). (*c*) Placement of gold bumps through the openings in the cable with a thermosonic ball bonder; (*d*) filling of the gap between cable and probe with epoxy and sealing of the gold bumps with silicone.

the ribbon cable are aligned to the corresponding contact pads on the silicon structure, which may be a probe or a platform. Then, using a ball bonder, gold bumps are pressed on the contact pads through the circular openings in the cable. By applying ultrasonic power at a temperature of 120 °C, the gold bumps are welded to the contact pads as indicated in figure 6(*c*). In this way, the electrical and mechanical connections are ensured simultaneously. The gap between the cable and the probe or platform is filled with the low-viscosity biocompatible n-butyl ester cyanoacrylate *Vetbond* from 3M, St Paul, USA, by capillary forces. The medical grade silicone *MED*-1000 from NuSil Technology, Carpinteria, USA, is applied in the last step to seal the gold bumps as illustrated in figure 6(*d*). The connection of the cable to a miniaturized connector or a printed circuit board (PCB) is performed in the same way. Details of the fabrication of the ribbon cable and the assembly are described elsewhere [22].

Examples of assembled systems for acute and sub-chronic applications are shown in figure 7. Figures 7(*a*) and (*b*) show a single probe with a 4 mm long shaft and nine electrodes for acute recording, and a four-shaft probe with 8 mm long shafts with a flexible cable connecting the 36 electrodes to a miniature connector, respectively. Figure 7(*c*) shows a combination of two 8 mm long probes to a 2 × 4 array with 72 electrodes attached directly to two flexible ribbon cables with miniature connectors. Finally, a platform-based array of 4 × 4 probes with 80 electrodes connected via a flexible ribbon cable to a PCB carrying two miniature connectors is shown in figure 7(*d*).

The cable-based assemblies can be applied in combination with a thin guide wire attached to a stereotaxic device. Alternatively, it can be used as a floating device easily following the brain movement in view of the high mechanical flexibility of the ribbon cable [20].

The assembly of the combs into a slim, platform-based 3D-electrode array is performed using a flip-chip bonder with an alignment accuracy of about 1 μm. Details of the fabrication process of the platform and the respective assembly procedure illustrated in figure 8 are given in [23]. In a first assembly step, a highly flexible ribbon cable is attached to the platform using the *MicroFlex* technology. The result

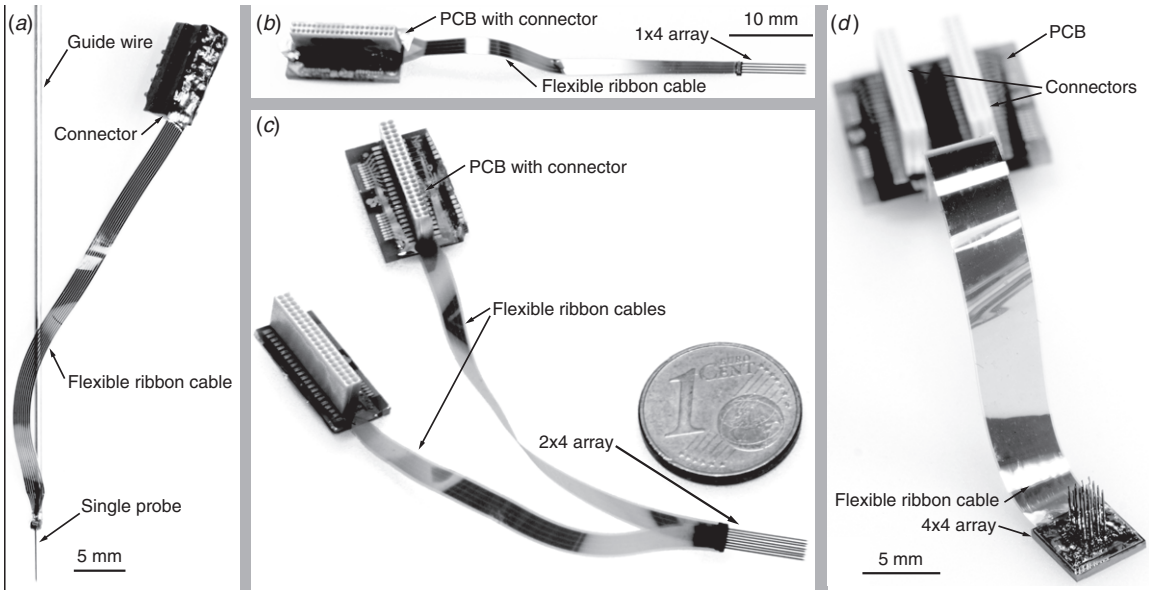

Figure 7. Photographs of (*a*) a single probe with 4 mm long shaft and nine electrodes attached to a guide wire for acute recording, (*b*) a four-shaft probe with 8 mm long shafts with a flexible cable connecting the 36 electrodes to a miniature connector, (*c*) a combination of two 8 mm long probes into a 2 × 4 array with 72 electrodes attached directly to two flexible ribbon cables with miniature connectors and (*d*) platform-based array of 4 × 4 probes with 80 electrodes connected via a flexible ribbon cable to a PCB comprising two miniature connectors.

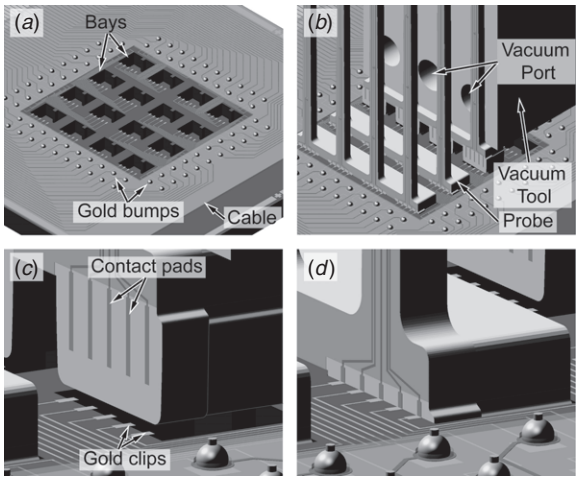

Figure 8. Assembly procedure of probe combs into the platform using a flip-chip bonder: (*a*) ribbon cable attached using the *MicroFlex* technology; (*b*) the probes are inserted with a vacuum tool into the bays of the platform; enlarged view of the probe base (*c*) before and (*d*) after insertion. The overhanging gold clips are bent down upon comb insertion. The electrical contact between electroplated contact pads and gold clips is achieved by mechanical caulking.

is shown in figure 8(*a*). Then, probe combs as shown in figure 2(*b*) are inserted into the bays of the silicon platform. This step is performed with a custom made vacuum tool attached to the flip-chip bonder as indicated in figure 8(*b*). The bays comprise overhanging gold clips 20 μm wide, 32.5 μm long and 4 μm thick [21]. Upon insertion of probe combs into the bays, the contact pads on the probes are pressed against these gold clips and the electrical and mechanical interconnection is achieved. The enlarged views of the probe base before and after insertion are presented in figures 8(*c*) and (*d*). The electroplated, protruding contact pads with heights between 3.5 μm and 4.1 μm were found to maintain a lower contact resistance of about 0.3 Ω per contact in comparison to planar Au pads (1.5 Ω per contact) and a higher assembly yield [23]. Figure 9 shows an optical micrograph of probe combs assembled in a platform with attached flexible cable. The height of the assembled system excluding the probe shafts measures 425 μm; the lateral dimensions do not exceed 5 × 5 mm^2. This is comparable to the highly compact array reported in [8]. While the backbone of the system reported in [5] is rather tall due to the monolithic integration of integrated circuits (IC) for signal processing on the probe base, more recent achievements of the same group demonstrated height [6, 7] and footprint [7] shrinkage by folding the IC parallel to the platform [6] or through hybrid integration of CMOS circuitry in the platform [7]. Our system might be extended through hybrid integration of a CMOS chip on the backside of the platform similar to [9]. This however would result in an increase in the footprint.

4. Experimental results

The electrodes are electrochemically characterized before *in vivo* experiments by measuring the electrode impedances

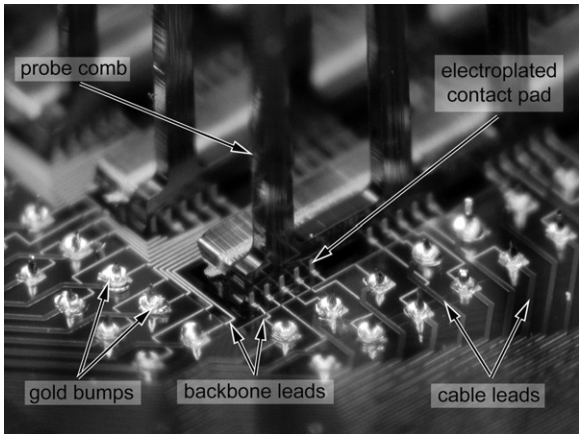

Figure 9. Optical micrograph of the assembled platform with four probe combs and flexible ribbon cable fixed through gold bumps.

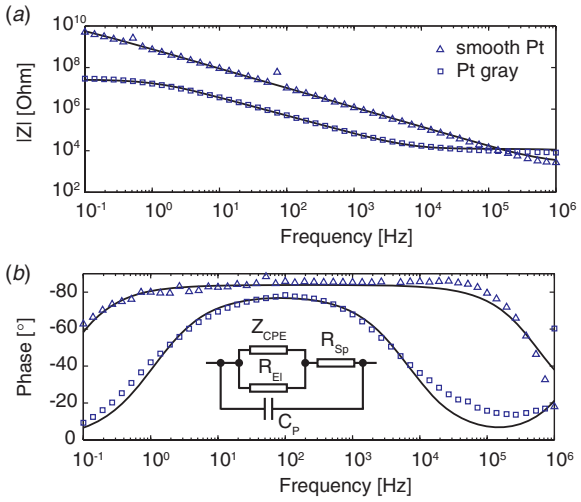

Figure 10. Measured characteristics of smooth Pt (triangles) electrodes in comparison to Pt gray (squares) electrodes. Together with the corresponding fits (solid lines) based on the electrical model as given with the inset in (*b*). Applied model values for the smooth Pt electrodes: $R_{El} = 1.3 \times 10^{10}$ Ω, $Z_{CPE} = 2.3 \times 10^{-10}$ (Hz Ω^{-1})$^{-n}$ with $n = 0.93$, $R_{Sp} = 3 \times 10^3$ Ω and $C_P = 5 \times 10^{-12}$ F. Applied model values for Pt gray electrodes: $R_{El} = 2.61 \times 10^7$ Ω, $Z_{CPE} = 7 \times 10^{-9}$ (Hz Ω^{-1})$^{-n}$ with $n = 0.88$, $R_{Sp} = 1.2 \times 10^4$ Ω and $C_P = 5 \times 10^{-12}$ F.

in a 0.9% saline solution at frequencies between 0.1 Hz and 1 MHz using the portable electrochemical interface and impedance analyzer *CompactStat*, from Ivium Technologies, the Netherlands, in a three-electrode configuration. Typical impedances for smooth Pt electrodes are between 1 MΩ and 2 MΩ at 1 kHz. As an alternative, platinum gray is electrochemically deposited [26] onto the electrodes to reduce their impedance. Figures 10(*a*) and (*b*) show the absolute value $|Z|$ and phase ϕ of the measured and modeled impedances of smooth Pt and Pt gray electrodes. The applied model is included in figure 10(*b*). It considers an electrode resistance R_{El} in parallel to a constant phase element Z_{CPE}, both in series with a spreading resistance R_{Sp}. Parasitic capacitive paths are taken into account by a parallel capacitor C_P. It is clearly recognizable at 1 kHz that the Pt gray electrodes exhibit an

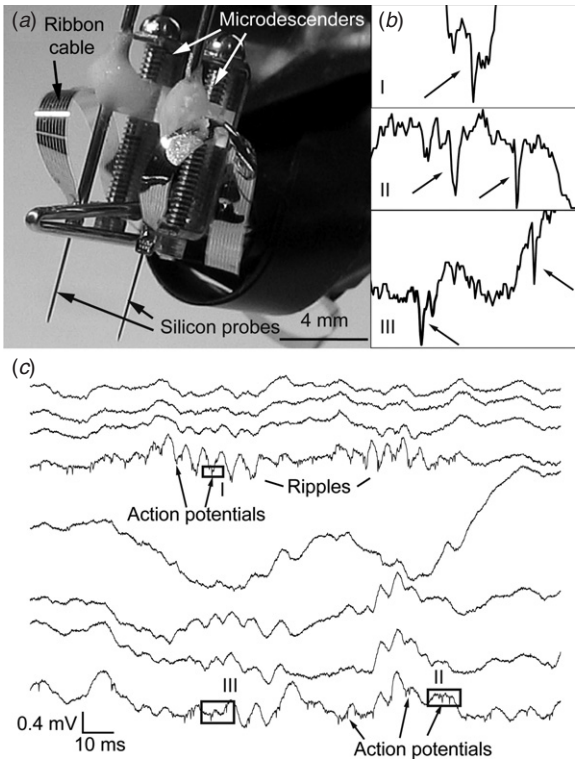

Figure 11. (*a*) Photograph of silicon probes mounted on micro-descenders used for adjustment of electrodes' positions; (*b*) enlarged views of action potentials at positions indicated by I, II and III in (*c*); (*c*) recorded signals from eight electrodes of one probe shaft, showing single action potentials and local field potentials.

impedance at least one order of magnitude lower than smooth Pt electrodes.

In vivo recordings in rats were conducted to prove the recording ability of the fabricated electrode arrays. Two 4 mm long single-shaft probes with nine Pt electrodes per shaft and 200 μm inter-electrode distances were bilaterally implanted into the hippocampus of an anesthetized rat after opening the dura mater. The recordings from unrestrained, sleeping rats started 1 week after surgery. Micro-descenders, shown in figure 11(*a*), are used to adjust the electrode positions by means of miniature screws during the experiments. The recorded signals presented in figure 11(*c*) were amplified by a factor of 1000 and filtered by a bandpass ranging from 1 Hz to 9 kHz. Fast oscillations of the local field potentials (LFP) termed ripples, with superimposed action potentials (AP), were observed on several channels for at least 15 days, as illustrated by the insets I, II and III in figure 11(*b*). These ripples occur during slow wave sleep or during resting phases of the awake animal. The results substantiate the ability of the fabricated probes to record LFP as well as AP for more than 2 weeks of implantation.

5. Discussion and conclusion

This paper presented silicon-based probe arrays fabricated using DRIE of standard silicon wafers. The described fabrication process is robust enough for batch fabrication. A thin-film metallization layer was evaporated and patterned by lift-off to realize electrodes, contact pads and interconnection leads. We applied an efficient method to pattern unique identifiers on the individual structures by adding a single lithography mask and few additional exposure steps. The introduced wafer code enabled the tracking of fabrication batches requiring a minimal area of 80 $\times$ 80 μm^2 only. Stress compensated dielectric layers were applied for insulation of the metallization, as a mask for the DRIE and as the passivation of the probes. Contact pads as thick as 4 μm were produced by application of wafer level electroplating. They ensure a high yield interconnection to the platform with a low contact resistance of 0.3 Ω per contact.

The fabrication technology reported here implements several improvements over the previous technology variant [19]. The improvements have lead to a more controlled probe fabrication with significantly higher yield, increased from typically 60% in the previous case to currently 100%, and have enabled the mentioned unique identification of each probe. The yield enhancement resulted from the improved coupling of the probe wafer to the support wafer and from the changed order of fabrication steps in comparison with the previous process [19].

The probes are compatible with multi-functional devices developed in the framework of the *NeuroProbes* project [15, 16]. It was demonstrated that they can be assembled into 1D, 2D and 3D probe arrays using two alternative techniques, namely interconnection to highly flexible ribbon cables or insertion into a slim platform. The electrodes were electrochemically characterized and showed impedances between 1 and 2 MΩ at 1 kHz for smooth Pt. By deposition of Pt gray the impedance was reduced by one order of magnitude. *In vivo* experiments with rats were conducted where APs as well as LFPs were recorded over the duration of at least 15 days. The presented results demonstrate excellent recording capability as well as a high mechanical stability of the fabricated probes.

The realized probe assemblies combine a range of advantages over previously reported devices, while avoiding the possible drawbacks of each of those. These advantages include high-yield fabrication as mentioned above, a sufficient robustness of the probe shanks needed for successful insertion, smooth shank sidewalls needed for minimally invasive insertion, fabrication using low-cost standard wafers, small overall thickness of the platform backbone beneficial for potential chronic implantation and sufficiently low electrode impedance for reliable neural signal acquisition.

Probe systems presented by researchers at the University of Michigan realize practically all of these advantages [5–7], with integration into three-dimensional arrays and platforms of similar thickness. An exception, however, is the higher fragility of probe shanks realized by strong boron doping, with typical thicknesses of 15 μm [3, 4]. The very smooth sidewalls of these shanks lend themselves for easy insertion [27]. Nevertheless, due to the tendency of the probes to buckle under axial forces [5], insertion across the dura mater proves

challenging. With the probes presented here, even transdural insertion is possible.

Moreover, the DRIE technology reported here enables the realization of probe shanks with the desired thicknesses suitable for various neuroscientific studies. Other DRIE-based approaches of neural probe fabrication have produced similar probe structures with comparable freedom of design. However, in the case where a standard wafer material was used [11], the shank sidewalls have obviously been quite rough. In the case where SOI was used, similarly smooth sidewalls have been reported [10, 12] and the thickness is precisely defined, however, at a significantly higher substrate cost. The probes and assemblies reported here are currently being used in various animal models by the different neuroscientific partners of the NeuroProbes project [13, 14].

Acknowledgments

The authors gratefully acknowledge Dominik Moser (IMTEK-MML) for assistance in system assembly, Kay Steffen (IMTEK-PRO) for support in electroplating, Birthe Rubehn (IMTEK-BMT) for assistance in cable fabrication, Joao Gaspar (IMTEK-MML) for advice in stress compensation of the dielectric thin films, and Michael Reichel and Armin Baur (both IMTEK-RSC) for technical support during clean room processing. The work was financially supported by the Information Society Technologies (IST) Integrated Project NeuroProbes of the 6th Framework Program (FP6) of the European Commission (project number IST-027017).

References

[1] Schmidt E M 1999 Electrodes for many single neuron recordings *Methods for Neural Ensemble Recordings* ed M A L Nicolelis (New York: CRS Press)

[2] Ulbert I, Halgren E, Heit G and Karmos G 2001 Multiple microelectrode-recording system for human intracortical applications *J. Neurosci. Methods* **106** 69–79

[3] Wise K D, Angell J B and Starr A 1970 An integrated-circuit approach to extracellular microelectrodes *IEEE Trans. Biomed. Eng.* **17** 238–47

[4] Najafi K, Wise K D and Mochizuki T 1985 A high-yield IC-compatible multichannel recording array *IEEE Trans. Electron. Devices* **32** 1206–11

[5] Bai Q, Wise K D and Anderson D A 2000 A high-yield microassembly structure for three-dimensional microelectrode arrays *IEEE Trans. Biomed. Eng.* **47** 281–9

[6] Yao Y, Ning Gulari M, Wiler J A and Wise K D 2007 A microassembled low-profile three-dimensional microelectrode array for neural prosthesis applications *J. Microelectromech. Syst.* **16** 977–88

[7] Perlin G E and Wise K D 2009 Ultra-compact integration for fully-implantable neural microsystems *Dig. Tech. Papers IEEE MEMS 2009 Conf. (Sorrento, Italy)* pp 228–31

[8] Campbell P K, Jones K E, Huber R J, Horch K W and Normann R A 1991 A silicon-based, three-dimensional neural interface: manufacturing processes for an intracortical electrode array *IEEE Trans. Biomed. Eng.* **38** 758–68

[9] Harrison R R, Watkins P T, Kier R J, Lovejoy R O, Black D J, Greger B and Solzbacher F 2007 A low-power integrated circuit for a wireless 100-electrode neural recording system *IEEE J. Solid-State Circuits* **42** 123–33

[10] Norlin P, Kindlundh M, Mouroux A, Yoshida K and Hofmann U G 2002 A 32-site neural recording probe fabricated by DRIE of SOI substrates *J. Micromech. Microeng.* **12** 414–9

[11] Pang C, Cham J G, Nenadic Z, Musallam S, Tai Y-C, Burdick J W and Andersen R A 2005 A new multi-site probe array with monolithically integrated parylene flexible cable for neural prostheses *Proc. IEEE Eng. in Med. and Biol. 2005 (Shanghai, China)* pp 7114–7

[12] Cheung K C, Djupsund K, Dan Y and Lee L P 2003 Implantable multichannel electrode array based on SOI technology *J. Microelectromech. Syst.* **12** 179–84

[13] Neves H P, Orban G A, Koudelka-Hep M and Ruther P 2007 Development of multifunctional probe arrays for cerebral applications *Proc. 3rd Int. IEEE EMBS Conf. on Neural Eng. (Kohala Coast, HI, USA, 2007)* pp 104–9

[14] Ruther P *et al* 2008 The NeuroProbes project—multifunctional probe arrays for neural recording and stimulation *Biomed. Tech.* **53** suppl 1 238–40

[15] Spieth S, Schumacher A, Seidl K, Hiltmann K, Haeberle S, Ruther P, McNamara R, Dalley J W, Edgley S A and Zengerle R 2008 Robust microprobe systems for simultaneous neural recording and drug delivery *IFMBE Proc. Europ. Biomed. Eng. Congress (Antwerp, Belgium, 2008)* vol 22 pp 2426–30

[16] Frey O, van der Wal P, de Rooij N and Koudelka-Hep M 2007 Development and characterization of choline and glutamate biosensor integrated on silicon microprobes for *in-vivo* monitoring *EMBC Proc. 29th Annu. Int. Conf. IEEE Eng. in Med. and Biol. Soc. (2007)* pp 6039–42

[17] Neves H P, Torfs T, Yazicioglu R F, Aslam J, Aarts A A A, Merken P, Ruther P and Van Hoof C 2008 The NeuroProbes project: a concept for electronic depth control *30th Int. IEEE EMBS Conf. 2008 (Vancouver, Canada)* p 1857

[18] Seidl K, Herwik S, Nurcahyo Y, Torfs T, Keller M, Schüttler M, Neves H P, Stieglitz T, Paul O and Ruther P 2009 CMOS-based high-density silicon microprobe array for electronic depth control on neural recording *Dig. Tech. Papers MEMS 2009 Conf.* pp 232-35

[19] Herwik S *et al* 2008 Fabrication technology for silicon based microprobe arrays used in acute and subchronic neural recording *Proc. 19th Workshop on Micro Mechanics Europe (Aachen, Germany)* pp 57–60

[20] Kisban S, Janssen P, Herwik S, Stieglitz T, Paul O and Ruther P 2008 Hybrid microprobes for chronic implantation in the cerebral cortex *30th Ann. Intern. IEEE EMBS Conf. (2008)* pp 2016–19

[21] Aarts A A A *et al* 2008 3D slim-base probe array for *in-vivo* recorded neuron activity *30th Annu. International IEEE EMBS Conf. (Vancouver, BC, Canada, 2008)* pp 5798–801

[22] Meyer J-U, Stieglitz T, Scholz O, Haberer W and Beutel H 2001 High density interconnects and flexible hybrid assemblies for active biomedical implants *IEEE Trans. Adv. Packag.* **24** 366–74

[23] Aarts A A A, Neves H P, Puers R P and Van Hoof C 2008 Interconnect for out-of-plane MEMS assembly *Proc. IEEE Intern. Interconn. Techn. Conf. (2008)* pp 132–4

[24] Gaspar J, Ruther P and Paul O 2007 Mechanical characterization of thin-film composites using the load-deflection response of multilayer membranes—elastic and fracture properties *Mater. Res. Soc. Symp. Proc.* **977** FF08

[25] Gaspar J, Schmidt M, Held J and Paul O 2008 Reliability of MEMS materials: mechanical characterization of thin-films

using the wafer scale bulge test and improved microtensile techniques *Mat. Res. Soc. Symp. Proc.* **1052** 1052-DD01-02

[26] Zhou D M 2007 Platinum electrode surface coating and method for manufacturing the same *US Patent* PCT/US2006/036966, WO/2007/050212

[27] Vetter R J, Miriani R M, Casey B E, Kong K, Hetke J F and Kipke D R 2005 Development of a microscale implantable neural interface (MINI) probe system *27th Annu. Intern. IEEE EMBS Conf. (Shanghai, China, 2005)* pp 7341–4